NEOPLASIA
www.neoplasia.com

Volume 13 Number 6 June 2011 pp. 537–549 **537**

Trimodal Glioblastoma Treatment Consisting of Concurrent Radiotherapy, Temozolomide, and the Novel TGF-β Receptor I Kinase Inhibitor LY2109761[1,2]

Mengxian Zhang[*,†,‡,3], Tobias W. Herion[†,3], Carmen Timke[†], Na Han[*], Kai Hauser[†], Klaus J. Weber[‡], Peter Peschke[†], Ute Wirkner[†], Michael Lahn[§] and Peter E. Huber[†,‡]

*Department of Oncology, Tongji Hospital, Tongji Medical College, Huazhong University of Science & Technology, Wuhan, China; [†]Department of Radiation Oncology, German Cancer Research Center, Heidelberg, Germany; [‡]Department of Radiation Oncology, University Hospital Center, Heidelberg, Germany; [§]Oncology Early Clinical Investigation, Lilly Research Laboratories, Indianapolis, IN, USA

Abstract

Here we investigate the effects of the novel transforming growth factor-β receptor I (TGF-βRI) serine/threonine kinase inhibitor LY2109761 on glioblastoma when combined with the present clinical standard combination regimen radiotherapy and temozolomide (TMZ). Human GBM U87 (methylated MGMT promoter), T98 (unmethylated MGMT promoter), and endothelial cells (HUVECs) were treated with combinations of LY2109761, TMZ, and radiation. We found that LY2109761 reduced clonogenic survival of U87 and T98 cells and further enhanced the radiation-induced anticlonogenicity. In addition, LY2109761 had antimigratory and antiangiogenic effects in Matrigel migration and tube formation assays. *In vivo*, in human xenograft tumors growing subcutaneously on BALB/c *nu/nu* mice, LY2109761 delayed tumor growth alone and in combination with fractionated radiation and TMZ. Interestingly, as expected, the methylated U87 model was more sensitive to TMZ than the unmethylated T98 model in all experiments, whereas the opposite was found for LY2109761. Moreover, with respect to tumor angiogenesis, while LY2109761 decreased the glioblastoma proliferation index (Ki-67) and the microvessel density (CD31 count), the relative pericyte coverage (α-SMA/CD31 ratio) increased in particular after triple therapy, suggesting a vascular normalization effect induced by LY2109761. This normalization could be attributed in part to a decrease in the Ang-2/Ang-1 messenger RNA ratio. LY2109761 also reduced tumor blood perfusion as quantified by noninvasive dynamic contrast-enhanced magnetic resonance imaging. Together, the data indicate that the addition of a TGF-βRI kinase inhibitor to the present clinical standard (radiation plus TMZ) has the potential to improve clinical outcome in human glioblastoma, especially in patients with unmethylated MGMT promoter status.

Neoplasia (2011) 13, 537–549

Abbreviations: DCE-MRI, dynamic contrast-enhanced magnetic resonance imaging; DEF, dose enhancement factor; GBM, glioblastoma multiforme; HUVEC, human umbilical vein endothelial cell; MGMT, O^6-methylguanine methyltransferase; MVD, microvessel density; RT, radiation therapy; TGF-βRI, transforming growth factor β receptor I; TMZ, temozolomide

Address all correspondence to: Peter E. Huber, MD, PhD, Department of Radiation Oncology, German Cancer Research Center (DKFZ)/University of Heidelberg Medical Center, 280 Im Neuenheimer Feld, Heidelberg 69120, Germany. E-mail: p.huber@dkfz.de

[1]This work was supported in part by grants from Deutsche Krebshilfe 106997, DFG National Priority Research Program the Tumor-Vessel Interface (SPP1190), Kompetenzverbund Strahlenforschung (KVSF, 03NUK004A, C) of Bundesministerien fuer Bildung, Forschung und Umwelt (BMBF/BMU), and the Tumorzentrum Heidelberg-Mannheim/NCT Heidelberg.

M.L. is an employee of Lilly, Inc, Indianapolis, IN. P.E.H. received a research grant from Lilly, Inc., Indianapolis, IN.

[2]This article refers to supplementary materials, which are designated by Tables W1 and W2 and are available online at www.neoplasia.com.

[3]These authors share first authorship.

Received 2 February 2011; Revised 6 April 2011; Accepted 7 April 2011

DOI 10.1593/neo.11258

Introduction

Glioblastoma multiforme (GBM) is the most common and the most malignant primary brain tumor in adults with a high degree of morbidity and mortality [1]. Despite intensive conventional treatment protocols, the prognosis of this tumor is still dismal [2]. One strategy to improve treatment outcome is to add more specific signaling inhibitors to the nonsurgical standard treatment regimen of chemoradiotherapy with temozolomide (TMZ). A promising target candidate is the inhibition of transforming growth factor-β (TGF-β) signaling.

TGF-β is a multifunctional ubiquitous polypeptide cytokine that binds and activates a membrane receptor serine/threonine kinase complex. On TGF-β binding, the receptor complex phosphorylates the transcription factors Smad2 and Smad3, which then bind to Smad4 and accumulate in the nucleus, where they regulate transcription of target genes [3]. The tumor suppressor function of TGF-β signaling is well established [4,5]. However, in some tumor types, and specifically in high-grade glioma, TGF-β becomes an oncogenic factor [6,7] and acts as a highly potent suppressor of immune reactions [8], an inductor of angiogenesis [9], and a promoter of cell motility and malignant invasion. The overexpression of TGF-β ligands has been reported in various malignant entities, such as malignant glioma [10,11], pancreatic carcinoma [12,13], and colorectal carcinoma [14,15]. In human malignant glioma, elevated levels of TGF-β are associated with high tumor grade, advanced tumor stages, and poor disease prognosis [10,16]. By virtue of the pivotal role of TGF-β in malignant glioma, a novel approach has been developed for the treatment of high-grade glioma based on the specific inhibition of TGF-β signaling pathway. Several small-molecule inhibitors of the TGF-β receptor kinase have been developed as promising therapeutic tools for the treatment of malignant glioma [17]. LY2109761, a novel TGF-βRI inhibitor, has shown a SMAD2-selective inhibitory profile with antitumor activity in various tumor models, such as breast cancer [18], colorectal cancer [19], pancreatic cancer [20], and hepatocellular carcinoma [21]. However, to our best knowledge, no study has been reported about the effects of LY2109761 on glioblastoma in combination with other therapies.

Considering that chemoradiotherapy with TMZ is the standard treatment approach in GBM after primary diagnosis, the addition of a TGF-β inhibitor seems a promising approach in this setting. For the present studies, we hypothesized that combining external beam radiotherapy with a TGF-β inhibitor augments tumor cell radiosensitivity because tumors have been shown to release TGF-β after radiation resulting in increased resistance to radiation [22,23]. Another potential anticipated beneficial effect of a TGF-β inhibitor is the reduction of glioma cell migration because sublethal doses of photon irradiation have been shown to promote migration and invasiveness of glioma cells [24,25]. We hypothesized that TGF-β inhibition could counteract this undesirable biologic effect of radiotherapy. Finally, we also expected potential antiangiogenic effects of blocking TGF-β signaling because tumor-derived TGF-β has been shown to cooperate with angiogenesis-promoting factors [26], such as vascular endothelial growth factor (VEGF) and basic fibroblast growth factor (bFGF).

Here, we investigated *in vitro* and *in vivo* effects of the small-molecule TGF-βRI inhibitor LY2109761 in combination with radiotherapy ± TMZ. In addition to tumor response, we were primarily interested in parameters that characterize the microenvironment and tumor physiology. To this end, we applied noninvasive radiologic imaging and evaluated blood perfusion and tumor angiogenesis using quantitative magnetic resonance imaging (MRI). Overall, the study shows that the combination of LY2109761 with radiotherapy and TMZ seems to have promising antitumor activity and provides a rationale to evaluate this or similar strategies in clinical trials.

Materials and Methods

Cell Cultures and Treatment Conditions

Primary isolated human umbilical vein endothelial cells (HUVECs; Promocell, Heidelberg, Germany) were cultured up to passage 8. Cells were maintained in culture at 37°C with 5% CO_2 and 95% humidity in serum-reduced (5% fetal calf serum) modified Promocell medium supplemented with 2 ng/ml VEGF, 4 ng/ml bFGF. Human glioblastoma (U87MG) tumor cells (Tumorbank DKFZ Heidelberg, Germany) and fast-growing T98 [27] were cultured in Dulbecoo modified Eagle medium with 10% fetal calf serum. LY2109761 was kindly provided by Eli Lilly (Indianapolis, IN), constituted in dimethyl sulfoxide (10 mM), and stored at −20°C. TMZ (Essex Pharma, Munich, Germany) was constituted in dimethyl sulfoxide (100 mM) and stored at −20°C. Cell exposures with the drugs were performed 2 hours before irradiating with 6-MV x-rays (Mevatron; Siemens, Erlangen, Germany) at a dose rate of 2.5 Gy/min.

Clonogenic Assay

For clonogenic assays increasing numbers of cells (10^2 to 5×10^4) were plated in 25-cm^2 flasks (Becton Dickinson, Heidelberg, Germany), and exposed to compound(s) and irradiation followed by incubation at 37°C for 10 to 14 days. Colonies formed were stained with crystal violet (Sigma, Germany), those with at least 50 cells were counted by microscopic inspection, and plating efficiency as well as clonogenic survival was calculated. The linear quadratic equation was fitted to data sets to generate survival curves. Dose enhancement factor (DEF) for drugs was calculated at the 10% survival level (DEF0.1, control radiation dose divided by the treated radiation dose). DEF values greater than 1.0 indicate enhancement of radiosensitivity.

Proliferation Assay

A total of 1×10^5 HUVECs were seeded on 25-cm^2 collagen-coated flasks overnight at standard conditions followed by exposure with different treatments and thereafter incubated for another 72 hours, and the total number of living cells was counted after trypan blue staining.

Matrigel Invasion/Migration Assay

The invasion/migration of glioblastoma and endothelial cells *in vitro* was measured on Matrigel-coated (0.78 mg/ml) transwell inserts with 8-μm pore size (Becton Dickinson). Cells were trypsinized and 500 μl of cell suspension (1×10^5 cells/ml) per experiment were added to transwells in triplicate. Chemoattractant medium containing VEGF and bFGF (750 μl) was added to the lower wells. After 12 hours of incubation, cells that had invaded the underside of the membrane were fixed and stained with Diff-Quik II solution (Dade Behring AG, Germany) and sealed on slides. Migrating cells were counted under microscopy.

Tube Formation Assay

To evaluate *in vitro* angiogenesis activity, tube formation assays were performed with HUVEC. Twenty-four-well plates were coated

with 300 μl of Matrigel (Becton Dickinson). HUVECs (5×10^4 cells) were suspended in 500 μl of medium containing various concentrations of compound(s) and/or receiving 4 Gy of irradiation and then added on the polymerized Matrigel. After incubating at 37°C for 6 hours, cells were fixed and stained with Diff-Quik II reagents (Dade Behring AG, Germany), photographed, and counted.

Gene Expression Analysis by Quantitative Real-time Polymerase Chain Reaction

At 6 hours after treatment, U87MG cells were solubilized and homogenized in TRIzol (Invitrogen, Carlsbad, CA). Total RNA was isolated according to the manufacturer's instruction, and purity and integrity of the RNA were assessed with Agilent 2100 BioAnalyzer (Agilent Technologies, Palo Alto, CA). Then quantitative real-time polymerase chain reaction (PCR) was performed using QuantiTect Primer assay (Qiagen, Hilden, Germany) and QuantiTect SYBR Green RT-PCR Kit (no. 204243; Qiagen) on a LightCycler 480 instrument (Roche Diagnostics, Mannheim, Germany). The detection and quantification involved the following steps: reverse transcription at 50°C for 30 minutes, initial activation at 95°C for 15 minutes, followed by 40 cycles of denaturation at 94°C for 15 seconds, annealing at 55°C for 30 seconds, and extension at 72°C for 30 seconds. Fluorescence data collection was performed at the extension step at 72°C. The relative expression of the target genes was calculated by normalizing the C_p (crossing point) values with those of housekeeping gene *GAPDH*. All assays were performed in triplicates.

Xenograft Tumor Study in Mice

Animal studies were performed according to the rules for care and use of experimental animals and approved by the local and governmental Animal Care Committee instituted be the German Government (Regierungspraesidium, Karlsruhe). Human glioblastoma xenografts were established by injecting 5×10^6 U87MG or T98 cells subcutaneously (s.c.) into the right hind limb of 6- to 8 week-old BALB/c athymic nude mice (Charles River Laboratories, Sulzfeld, Germany). Tumor growth was followed until tumor volume reached approximately 150 mm^3 as measured with calipers and calculated by the formula: volume (V) = length (a) × width (b) × width (b) × 0.5. Then animals were randomized into eight groups (13-15 mice per group with three mice scheduled for histology after day 14 of treatment for the U87MG model and 8 to 10 mice per group for the T98 model): control, LY2109761 only, TMZ only, irradiation only, LY2109761 combined with TMZ, LY2109761 combined with radiation, TMZ combined with radiation, and LY2109761 combined with TMZ and radiation. Starting on day 0, TMZ was administered intraperitoneally (i.p.) in PBS at 50 mg/kg five times weekly. LY2109761 was dissolved in the NaCMC/SLS/PVP/antifoam oral vehicle (1% sodium carboxymethylcellulose, 0.5% sodium lauryl sulfate, 0.085% PVP, and 0.05% antifoam; Eli Lilly) and administered orally at 50 mg/kg twice daily (days 1-5 of each week) until the end of observation. Tumors were irradiated with a fractionated schedule (5 × 2 Gy) starting on day 0 for five consecutive days using a 6-MV LINAC (Siemens).

Immunohistochemistry

For histologic analysis, U87MG xenografts were harvested from three additional animals per treatment group, 10 days after the start of therapy. Cryostat tumor sections were stained with mouse anti-CD31 IgG2a antibody (1:100; BD Pharmingen, San Jose, CA) for 30 minutes at 37°C followed by staining with Alexa Fluor 555–labeled goat antimouse IgG2 antibody (1:400; Invitrogen) for 30 minutes at 37°C. Then the sections were incubated with rabbit anti–α-SMA antibody (1:100; Abcam, Cambridge, UK) for 30 minutes at 37°C and followed by incubation with Alexa Fluor 488–labeled antirabbit IgG2 antibody (1:400; Invitrogen) for 30 minutes at 37°C. Then mounting medium containing 4′,6 diamidino-2-phenylindole (Vector Laboratories, Burlingame, CA) was applied to stain all nuclei. Similarly, the Ki-67/4′,6 diamidino-2-phenylindole staining was performed. Primary antibody and dilution were as follows: Rabbit anti–Ki-67 (Abcam) at a concentration of 5 mg/ml digital fluorescent images were obtained using a Nikon Eclipse E600 microscope (Duesseldorf, Germany) equipped with a Nikon digital sight DS-U1 camera.

Dynamic Contrast-Enhanced Magnetic Resonance Imaging

MRI was performed on a clinical 1.5-T whole-body MRI system (Siemens Magnetom Vision) using a custom-made small-animal solenoid Tx/Rx radiofrequency coil. Dynamic contrast-enhanced (DCE) MRI was performed using a two-dimensional T1-weighted saturation recovery gradient echo sequence (saturation recovery turbo fast low angle shot, TR = 13 milliseconds, TE = 5.3 milliseconds, T_{REC} = 300 milliseconds, flip angle = 12°, matrix = 128 × 48, resolution = 0.5 × 0.5 × 2.0 mm^3, average = 4) [28]. A total number of 120 dynamic images were acquired with a temporal resolution of 7.5 seconds, resulting in a total scan time of 15 minutes. The contrast agent Gadomer (Bayer Schering Pharma, Berlin, Germany; molecular weight = 17 kDa; 0.05 mmol/kg diluted in 0.9% NaCl to a total volume of 100 μl) was injected manually through the tail vein (infusion time = 5 seconds). The DCE-MRI postprocessing was done based on the two-compartment model developed by Brix et al. [29] using Dynalab software (MeVis Research, Bremen, Germany). Functional parameters *amplitude A* (describes relative change in signal intensity after the contrast agent injection relative to precontrast values) as a measure for relative blood volume in the tumors and k_{ep} (describes the volume transfer constant between the extravascular extracellular space and the blood plasma) as a measure for fluid exchange between vasculature and extravascular space were calculated pixelwise, color-coded, and overlaid on the morphologic MR images.

Statistical Analysis

The unpaired two-tailed t test was used for the comparison of parameters between groups. The Kaplan-Meier method was used to determine the mean time to tumor progression (TTP), and a log-rank test was used to compare the differences between each treatment condition. A value of $P < .05$ was considered significant. The statistical analysis was performed using the software package Statistika 6.0 (Statsoft, Hamburg, Germany).

Results

Clonogenic Survival

Treatment of glioblastoma cells with increasing concentrations of LY2109761 and TMZ showed a dose-response relationship distinct for each cell line and each compound (Figure 1*A*). U87MG cells displayed greater sensitivity to TMZ exposure than T98 (Figure 1*A*, *left panel*). Conversely, T98 cells were markedly more sensitive to LY2109761 than U87MG cells (Figure 1*A*, *right panel*). Accordingly, the concentration of LY2109761 inducing a surviving fraction of

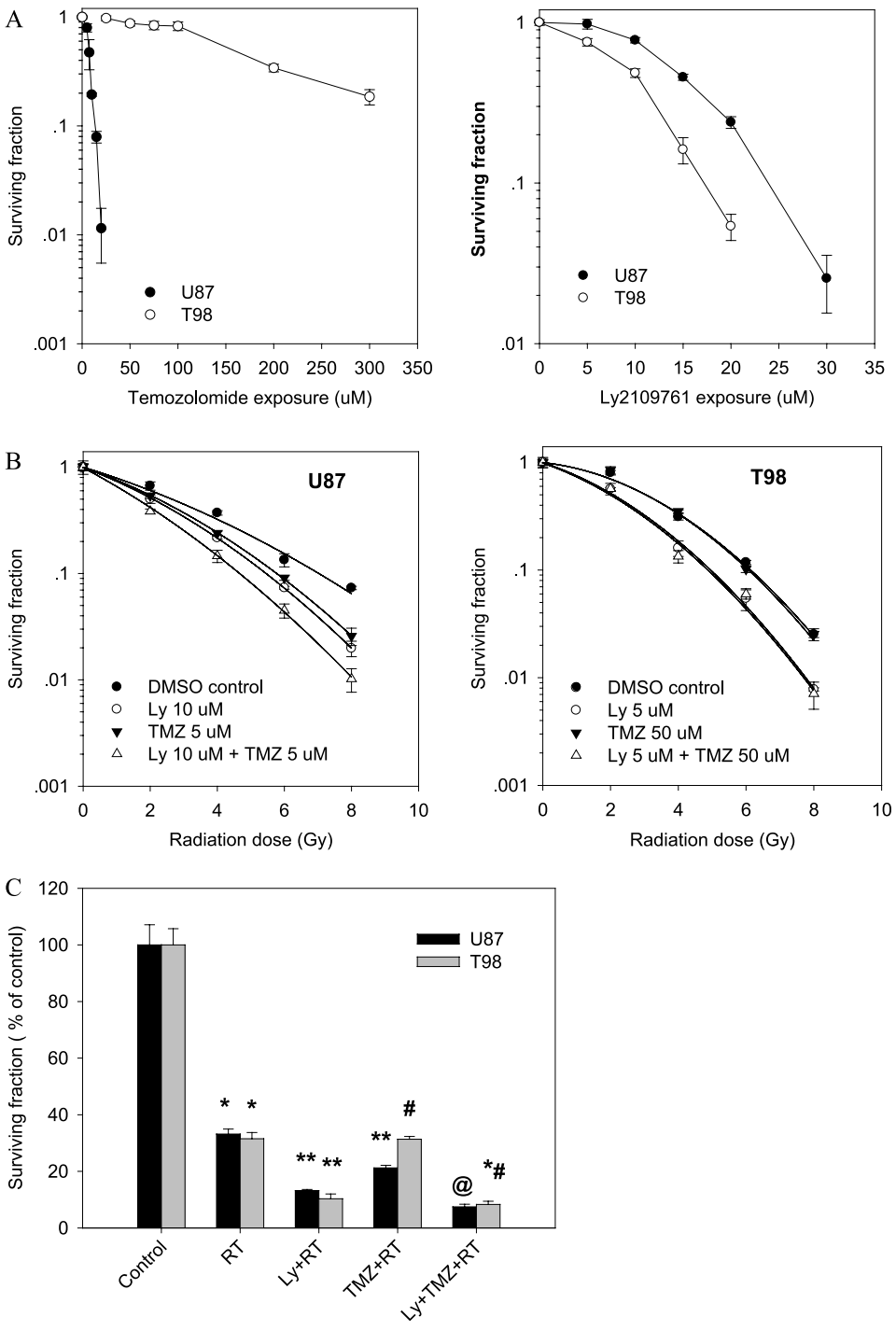

Figure 1. Clonogenic survival of glioblastoma cell lines after each treatment. (A) The effects of LY2109761 and TMZ exposures on the clonogenic survival of U87MG (left) and T98 (right). (B) The effects of LY2109761 and TMZ on the radiosensitivity of U87MG (left) and T98 (right). Bars indicate SD; Ly, LY2109761; points, mean; TMZ, temozolomide. (C) Detailed analysis of clonogenic survival for RT ± Ly ± TMZ in U87MG and T98 depicted as bars. All effects in this figure are normalized to the control experiment. Bars indicate ±SD; columns, mean; Ly, LY2109761 (10 μM for U87MG; 5 μM for T98); RT, radiation (4 Gy); TMZ, temozolomide (5 μM for U87MG; 50 μM for T98). *$P <$ .05 *versus* controls. **$P <$ .05 *versus* RT. $^{@}P <$ .05 *versus* RT, Ly + RT, and TMZ + RT. $^{\#}$Nonsignificant *versus* RT. *$^{\#}P <$ .05 *versus* TMZ + RT and nonsignificant *versus* Ly + RT.

~80% was approximately 10 μM for U87MG and 5 μM for T98, respectively. For subsequent combination clonogenic assay experiments, doses of LY2109761 and TMZ for moderate toxicity were used: U87MG = 10 μM LY2109761 and 5 μM TMZ; T98 = 5 μM LY2109761 and a TMZ concentration of 50 μM, which corresponds to the serum concentration achieved in humans using the standard protocol of 150 mg/m^2 per day [30].

Next we investigated whether LY2109761 and TMZ would act as radiosensitizers in glioblastoma cells. The surviving fraction was normalized for the cytotoxicity induced by the compound(s) and

the linear quadratic equation was fitted to data sets (Figure 1*B*). Both LY2109761 and TMZ showed radiosensitizing effects on U87MG cells with a DEF0.1 of 1.29 and 1.22, respectively. The combination of LY2109761 and TMZ further increased the radiosensitivity of U87MG cells with a DEF0.1 of 1.51 (Figure 1*B*, *left panel*, and *C* and Table W1). Whereas the addition of LY2109761 led to an increase of radiosensitivity in T98 cells (DEF0.1 = 1.24), no radiosensitizing effect was observed by TMZ and no further increase of radiosensitivity was achieved after the addition of TMZ to the combination treatment with LY2109761 and radiation in T98 cells (Figure 1*B*, *right panel*, and *C* and Table W1).

Endothelial Cell Proliferation

To investigate the effects of different treatment regimens on endothelial cell proliferation as the effector cells of angiogenesis, a cell count proliferation assay was performed in HUVEC. We found that each treatment (LY2109761 at 5 μM, TMZ at 50 μM, and radiation at 4 Gy) decreased the proliferation of HUVEC in a range of 40% to 60% ($P < .05$). Dual or triple combination treatment further reduced the cell number (Figure 3*A*, $P < .05$). Triple combination showed a superior inhibitory effect on endothelial cell proliferation compared with radiation and TMZ ($P < .05$).

Cell Invasion/Migration

To investigate the effects of different treatment regimens on glioblastoma and endothelial cell invasion/migration, Transwell invasion/migration assays were performed. We found that radiation (4 Gy) and/or TMZ (50 μM) treatment enhanced U87MG and HUVEC migration through the extracellular matrix (Matrigel) compared with control ($P < .05$). Importantly, LY2109761 (10 μM) strongly suppressed the constitutive and treatment-induced migration in U87MG and HUVEC ($P < .05$). There was no significant difference in the migratory cell number between each LY2109761 including regimen (Figures 2, *A* and *B*, and 3, *B* and *C*). In addition, transwell invasion/migration assays in T98 cells displayed similar results (data not shown).

Tube Formation

The sprouting of endothelial cells and formation of tubes are crucial steps in the angiogenic process. Control HUVEC spread and aligned with each other and formed a rich meshwork of branching anastomosing capillary-like tubules with multicentric junctions. This

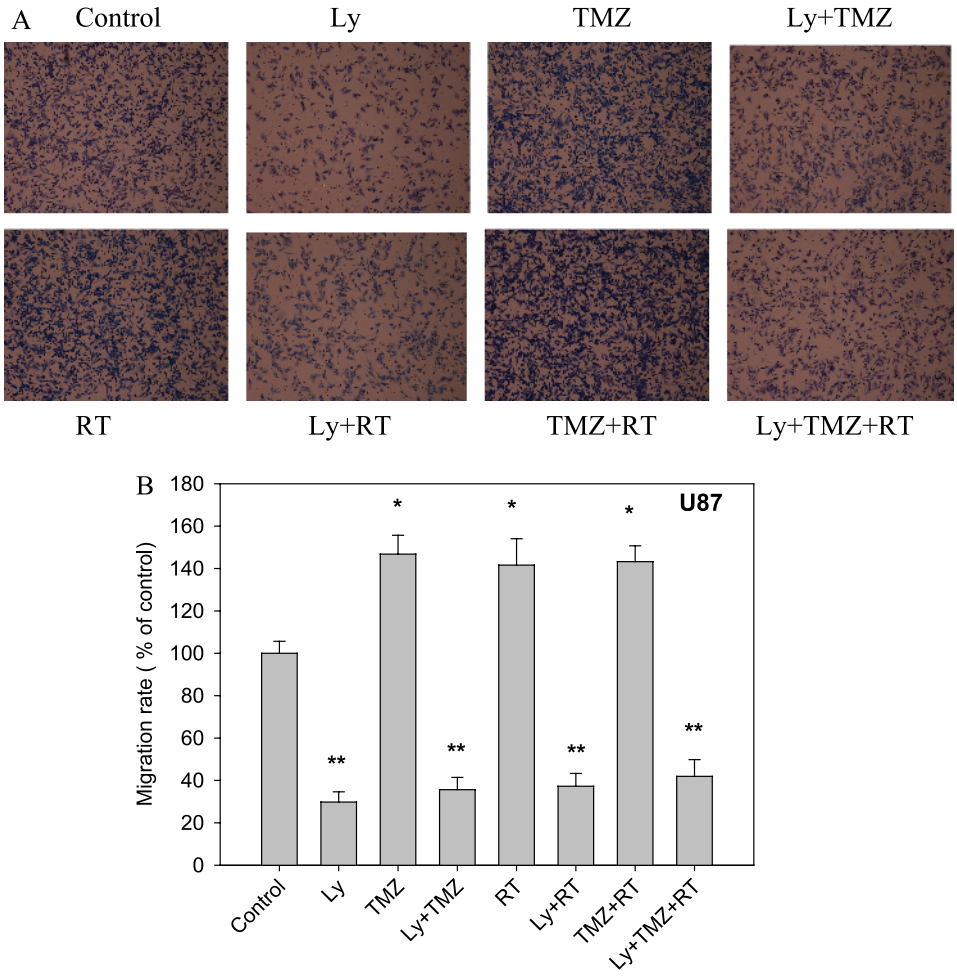

Figure 2. The effects of each treatment on tumor cell migration/invasion. U87MG cell migration/invasion was determined by counting cells that had migrated to the lower side of an invasion chamber 12 hours after treatment. (A) Stained cells in representative fields (100×). (B) The number of cells that had migrated shown as histogram: bars indicate SD; columns, mean; Ly, LY2109761 (10 μM); RT, radiation (4 Gy); TMZ, temozolomide (50 μM). *$P < .05$ *versus* control. **$P < .05$ *versus* control and treatment without LY2109761.

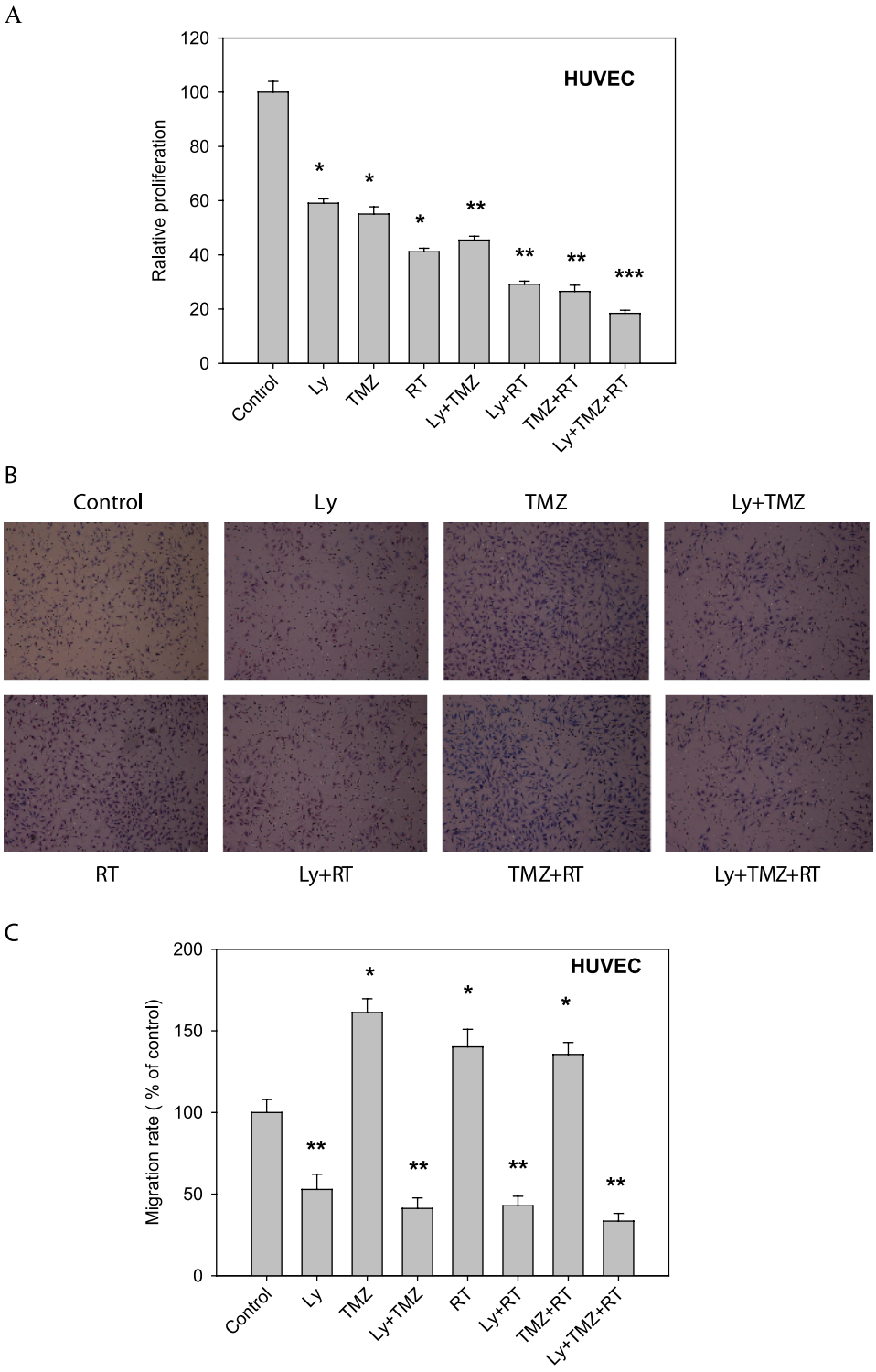

Figure 3. The effects of each treatment on endothelial cell proliferation, migration, and tube formation. (A) HUVEC proliferation was determined by cell count 72 hours after exposure to the following treatments: LY2109761 (Ly, 10 μM), TMZ (50 μM), radiation (RT, 4 Gy), the dual or triple combination. Relative number of cells is shown as a histogram: bars indicate SD; columns, mean. *$P < .05$ *versus* control. **$P < .05$ *versus* control and respective single treatment. ***$P < .05$ *versus* all other treatments. (B) HUVEC migration was determined by counting cells that had migrated to the lower side of an invasion chamber 12 hours after treatment. Stained cells in representative fields (100×). (C) The number of HUVEC that had migrated is shown as a histogram: bars indicate SD; columns, mean. *$P < .05$ *versus* control. **$P < .05$ *versus* control and treatment without LY2109761. (D) The ability of HUVEC to form tubule-like structures when plated on Matrigel was determined for cells in each treatment condition. Photographs of representative tube formation fields are shown (100×).

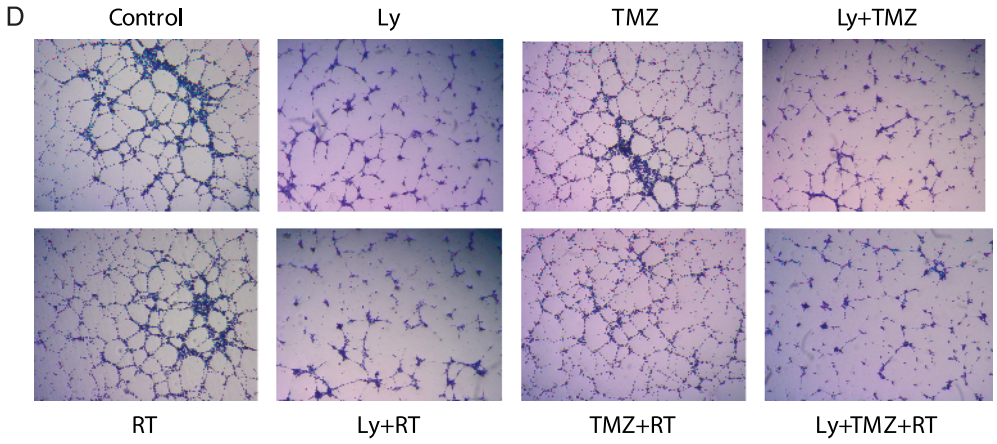

Figure 3. (*continued*).

process was hardly influenced by either radiation and/or TMZ. LY2109761 alone and in combination with radiation and/or TMZ reduced and disorganized the tube-like structures (Figure 3*D*).

Gene Expression Changes of Ang-1 and Ang-2

As shown for U87MG quantitative real-time polymerase chain reaction analysis revealed that the messenger RNA (mRNA) level of Ang-1 remained unchanged for all treatment conditions (Figure 4). However, LY2109761 (10 μmol) alone or in combination with TMZ (50 μmol) and/or radiation (4 Gy) significantly reduced Ang-2 mRNA expression, whereas a slight but not statistically significant increase of Ang-2 expression was documented after treatment with TMZ and radiation alone or their combination.

Glioblastoma Tumor Growth in Mice In Vivo

Next we determined whether the enhancement of antitumor effects of LY2109761 and TMZ *in vitro* could be translated into an *in vivo* tumor model. Tumor growth delay assays were performed in s.c. U87MG and T98 glioblastoma xenograft mouse models and the TTP, as defined by tumors reaching three times their baseline size [31], was calculated using the tumor volumes from the individual mice in each group. For U87MG tumors, as shown in Figure 5*A* and Table W2, animals of the control group showed a progressive increase of tumor volume with a mean TTP of only 11.1 ± 1.79 days. All monotherapies resulted in significant tumor growth delay and subsequent prolonged TTP (radiation therapy (RT) = 29.7 ± 7.17 days, LY2109761 = 32.0 ± 6.28 days, TMZ = 64.3 ± 9.14 days). Radiation treatment plus LY2109761 or TMZ (RT + LY2109761 = 62.1 ± 8.29 days, RT + TMZ = 75.4 ± 8.29 days) was significantly more effective than the respective monotherapies ($P < .05$). The combination of LY2109761 and TMZ (79.9 ± 7.15 days) had a tendency to enhance tumor growth delay *versus* TMZ monotherapy, but this combinatorial effect was not marked and the difference was not statistically significant ($P > .05$). Importantly, the triple combination of all three therapies was significantly more effective than all other regimens showing the largest effect on tumor growth delay (95.9 ± 2.39 days). For T98 tumors, as shown in Figure 5*B* and Table W2, LY2109761 or radiation monotherapy induced marked tumor growth delay, with an increased mean TTP (RT = 20.9 ± 4.32 days, LY2109761 = 16.5 ± 2.53 days) compared with controls (10.2 ± 1.26 days). Their combination resulted in a further increased TTP (30.78 ± 6.16 days) in a supra-additive manner. However, no statistically significant increase of TTP was observed by TMZ monotherapy (11.9 ± 1.58 days) and no further increase of TTP was achieved after the addition of TMZ to LY2109761 or radiation or their combination.

Immunohistochemistry

The Ki-67 index in U87MG tumors as a global proliferation marker was reduced in all treated groups (Figure 6). Tumors after dual treatments had lower Ki-67 indices than after single therapies. Triple combination resulted in a further decrease of the Ki-67 index compared with all dual combinations ($P < .05$; Figure 6*B*). Antiangiogenic therapeutic effects in tumors can be associated with reduced microvessel density (MVD), and an increased ratio of α-SMA/CD31–positive tumor blood vessels after therapy indicates a tumor vascular normalization process. As shown in Figure 6*C* and *D*, a significant decrease in microvessel count (CD31) and an increase in the fraction of pericyte

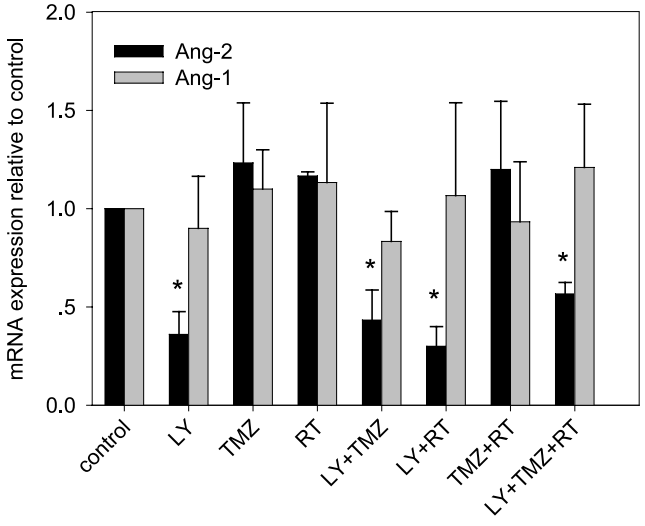

Figure 4. mRNA expression of Ang-1 and Ang-2 of U87MG cells in the different treatment conditions versus untreated controls. Bars indicate SD; columns, mean; Ly, LY2109761; RT, radiation; TMZ, temozolomide. *$P < .05$ *versus* control.

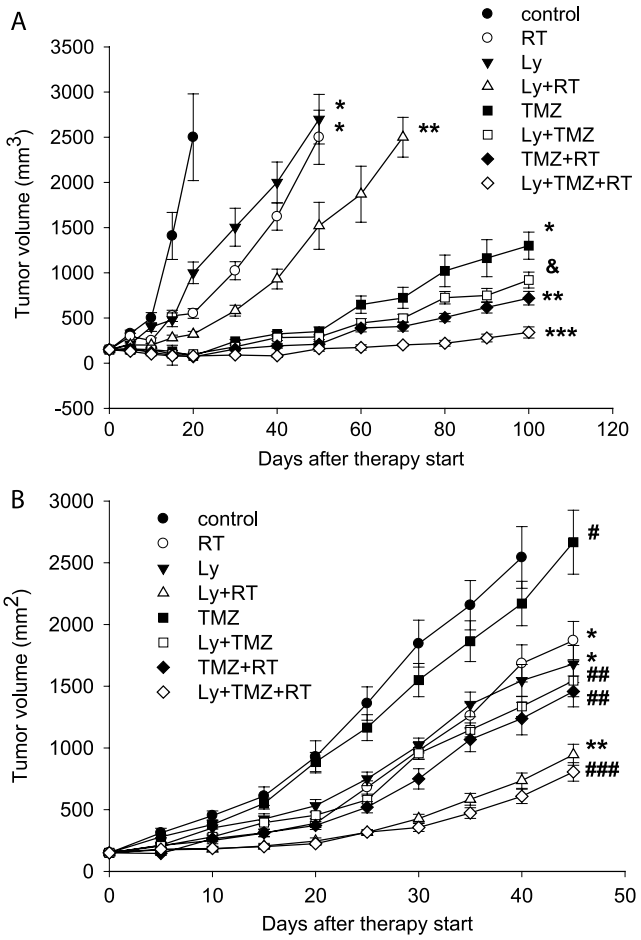

Figure 5. *In vivo* growth of U87MG and T98 tumor xenografts. BALB/c *nu/nu* mice with U87MG (A) and T98 (B) human glioblastoma growing s.c. were treated as described in Materials and Methods. Points: mean of tumor volume normalized to the day of therapy start (d0). Bars indicate SE. $^{*}P < .05$ *versus* control. $^{**}P < .05$ *versus* control and each monotherapy. $^{***}P < .05$ *versus* control, each monotherapy and dual therapy. $^{\&}P > .05$ *versus* TMZ monotherapy, $^{\#}P > .05$ *versus* control. $^{\#\#}P > .05$ *versus* control and each monotherapy. $^{\#\#\#}P > .05$ *versus* control, each monotherapy and dual therapy.

coverage (α-SMA/CD31) were observed after single treatment with LY2109761, TMZ, or irradiation ($P < .05$). Dual combinations with LY2109761 further reduced vessel count and increased pericyte coverage compared with single treatments ($P < .05$). The triple combination

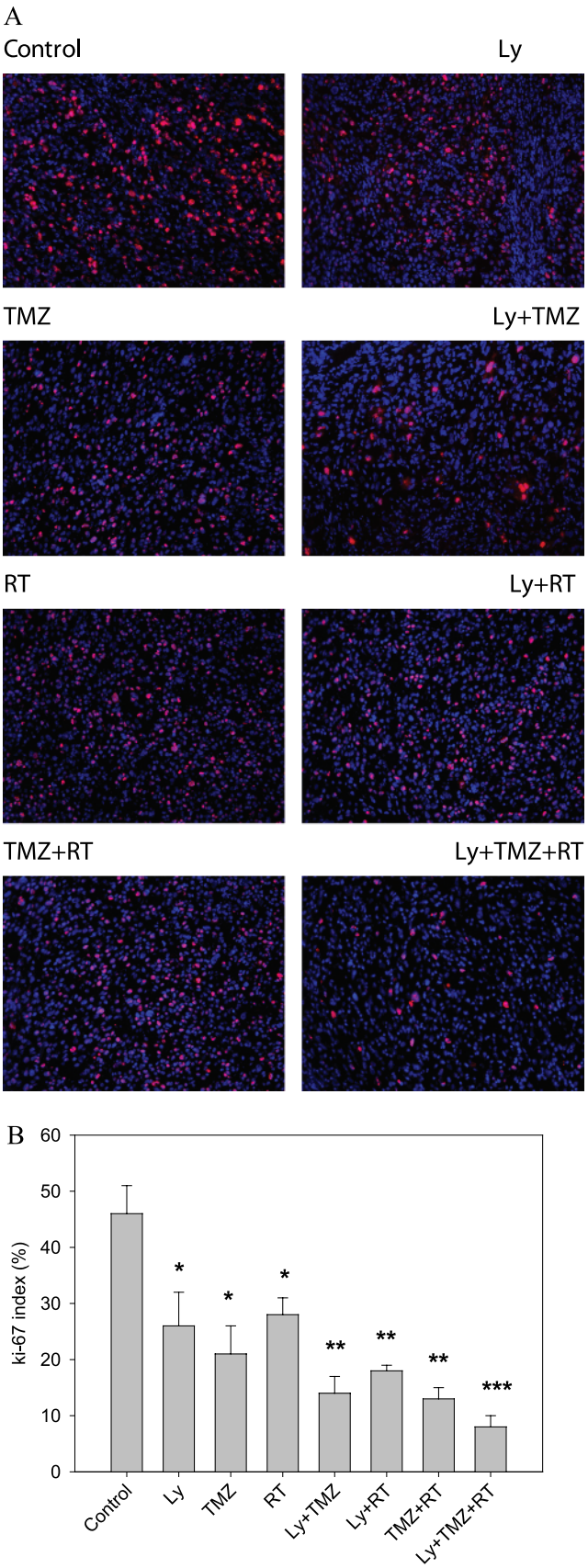

Figure 6. Immunohistochemical evaluation of each treatment on the proliferation and intratumoral vasculature within U87MG xenografts. Tumor-bearing mice were killed on days 14 after the start of treatment (three animals per group). Tumors were excised and processed as described in Materials and Methods. (A) Representative examples for the detection of Ki-67 in tumor sections from various treatment groups (200×). (B) Quantitative comparison of the Ki-67 index in the tumor sections from the eight groups of animals. (C) Representative examples for the double staining of CD31/α-SMA (red, CD31; green, α-SMA) in tumor sections from various treatment groups. Original magnification, ×200. (D) Quantitative comparison of tumor vessel (left panel) and fraction of pericyte coverage (right panel) in the tumor sections from the eight groups of animals. $^{*}P < .05$ *versus* control. $^{**}P < .05$ *versus* control and respective single treatment. $^{***}P < .05$ *versus* all other treatments. $^{*\#}P < .05$ *versus* Ly + RT and TMZ + RT but nonsignificant *versus* Ly + TMZ. Bars indicate SD; columns, mean.

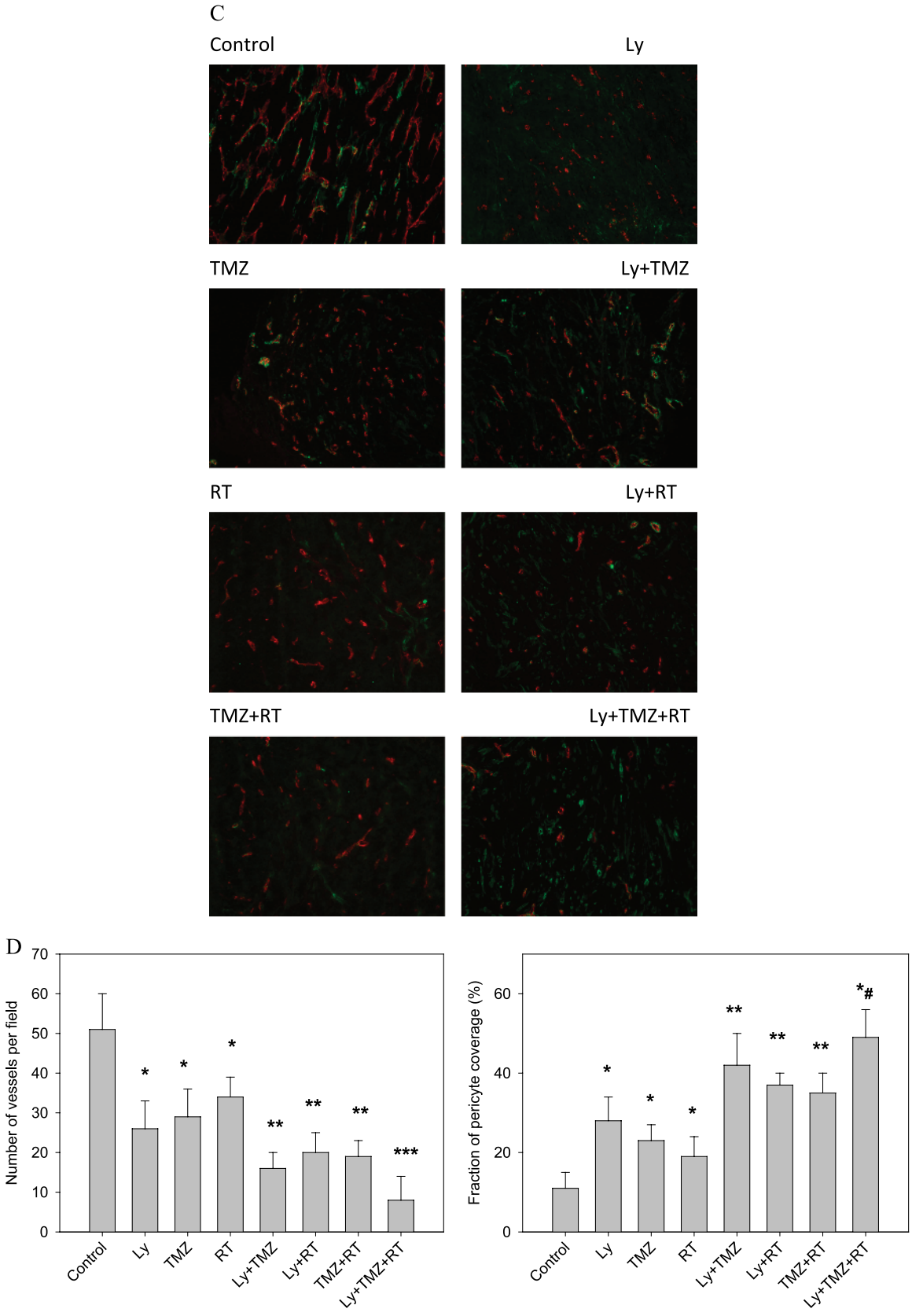

Figure 6. (*continued*).

showed the lowest vessel number and highest fraction of pericyte coverage compared with all other groups ($P < .05$).

In Vivo *Imaging of Tumor Blood Perfusion Using DCE-MRI*

To investigate the tumor perfusion, three U87MG tumor-bearing mice randomized to histologic examination from each group were subjected to DCE-MRI on day 14 directly before killing. *Amplitudes* and k_{ep} were measured in regions of interest covering the total tumor (Figure 7). A significant decrease in the *amplitude* level as a measure for tumor blood volume was observed under all monotherapies (LY2109761, TMZ, and RT) compared with the control group ($P < .05$). Combination treatments, both dual and triple, did not further decrease the *amplitude* value. Surprisingly, the exchange rate constant k_{ep}, which is a compound parameter highly influenced by vessel permeability, increased significantly after LY2109761 treatment ($P < .05$), whereas radiation and TMZ tended to decrease the exchange rate k_{ep}.

Discussion

The clinical prognosis for glioblastoma patients is still extremely poor. Almost all patients die with or without surgery and additional radiotherapy within 2 years from the diagnosis. The recent addition of the classic chemotherapeutic agent TMZ in various schedules concurrent to radiotherapy with later maintenance has only prolonged the median survival for a few months [2]. This situation rationalizes the search for an integration of suitable novel and effective drugs into the treatment. The inhibition of the TGF-β signaling pathway is considered a promising strategy in treating glioblastoma. One reason is that the overexpression of TGF-β is associated with proliferation, invasion/migration, and angiogenesis in glioma [10,11,16].

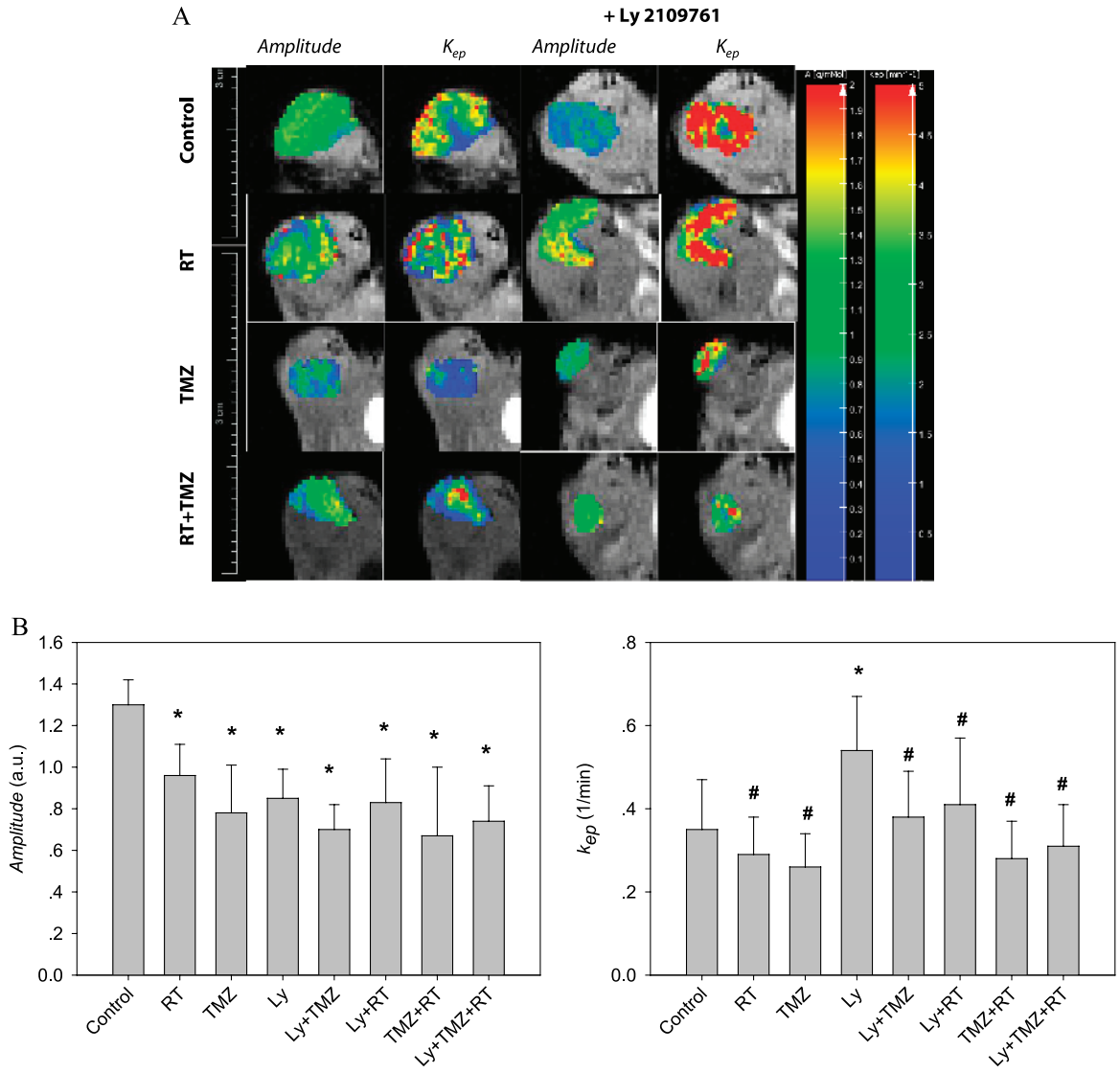

Figure 7. MRI with *amplitude* and k_{ep} parameters of U87MG tumors under different treatments. Three tumor-bearing mice from each group were subjected to DCE-MRI measurement on day 14 before histologic examination. *Amplitudes* and k_{ep} were measured in regions of interest covering the total tumor. (A) Representative examples of color-coded *amplitude* and k_{ep} parameter maps from different treatment groups. (B) Quantitative comparison of the *amplitude* (left panel) and k_{ep} (right panel) parameter of the tumor from the eight groups of animals. Bars indicate SD; columns, mean; Ly, LY2109761; RT, radiation; TMZ, temozolomide. *$P < .05$ *versus* control. #Nonsignificant ($P > .05$) *versus* control.

In the present study, we investigated a trimodal glioblastoma treatment regimen combining LY2109761, a novel TGF-βRI kinase inhibitor, with radiotherapy and the chemotherapeutic agent TMZ. We show that the addition of LY2109761 to fractionated radiation ± TMZ markedly increased the antitumor effect of the standard treatment in human glioblastoma *in vitro* and *in vivo*. The here suggested regimen can, in principle, be transferred into the clinic because the combination of radiotherapy with TMZ is the nonsurgical standard of care for most glioblastoma patients.

The beneficial combination effect is presumably based on multiple effects of LY2109761 on both tumor cells and the tumor microenvironment. Our *in vitro* data show that LY2109761 has both direct cytotoxic effects and radiosensitizing effects on glioblastoma cells (U87MG and T98). TMZ demonstrated significant cytotoxic and radiosensitizing effects on U87MG cells, even at low concentrations, whereas little such effects of TMZ were observed in T98 cells even at higher, clinically relevant concentrations. This differential response between these two glioblastoma cells to TMZ was also observed in our animal experiment, which can be explained by their difference in O^6-methylguanine methyltransferase (MGMT) methylation and expression status. It has been reported that the promoter of MGMT in U87MG glioblastoma is methylated and expression is low, whereas in T98 cells, the promoter of MGMT is unmethylated and thus the protein expression is positive [32,33]. The protective effect of MGMT activity against the cytotoxic effects of alkylating agents has been demonstrated in several human glioma cell lines [33,34] as well as in the clinical setting. Hegi et al. [35] reported that glioblastoma patients with unmethylated MGMT promoters did not seem to experience a survival benefit from the addition of TMZ to radiation. Importantly, in the present study, no protective effect of MGMT activity was observed against the antitumor effect of LY2109761. Conversely, the unmethylated T98 cells were found to be approximately 1.5-fold more sensitive to LY2109761 than the methylated U87MG at the 10% survival fraction end point. Furthermore, our *in vivo* data showed that the addition of LY2109761 markedly increased antitumor activity of radiotherapy ± TMZ, resulting in increased tumor growth delay in both MGMT-positive and -negative tumors. These data suggest that the combination of LY2109761 with chemoradiotherapy might be a promising multimodality treatment approach in glioblastoma, including for those patients whose tumors express MGMT and may therefore benefit less from TMZ.

Local invasive growth is a key feature of glioblastoma, and the high invasion/migration character is considered to be a major therapeutic obstacle for glioblastoma treatment. A number of signaling pathways can be constitutively activated in migrating glioma cells, rendering these cells resistant to cytotoxic insults [36,37]. Moreover, ionizing radiation has been reported to be able to promote tumor invasion/migration itself [24,38]. This context provides another rationale for the use of LY2109761 in glioblastoma treatment because we found that LY2109761 was able to reduce glioblastoma and HUVEC cell migration/invasion. More importantly, the addition of LY2109761 to radiotherapy ± TMZ also markedly reduced the treatment-induced invasion/migration of glioblastoma cells. These findings are in agreement with reports demonstrating the implication of TGF-β in glioma cell invasion and migration [39] and with findings showing that the inhibition of TGF-β signaling suppressed cell invasion/migration in glioma and other types of cancers [18–21,40]. Together, our data indicate that LY2109761 is a potent antimigratory compound for glioblastoma. The data also rationalize the addition of LY2109761 or a substance with similar properties to conventional radiotherapy and/or chemotherapy to counteract the potential undesired promigratory effect of radiotherapy.

The LY2109761 effects on tumor physiology, blood perfusion, and tumor angiogenesis provide another reason for the beneficial antitumor combination effects with radiation and TMZ *in vivo*. Antiangiogenic therapy has shown promise in the treatment of various types of cancers alone and in combination with conventional chemotherapy and/or radiotherapy [41,42]. In human glioma cells, TGF-β has been shown to be a potent inducer of VEGF and $\alpha_v\beta_3$ integrin expression [43,44], indicating that TGF-β signaling has a role in tumor angiogenesis [9,26]. Accordingly, we found that LY2109761 strongly inhibited proliferation and migration of endothelial cells and, consequently, disabled new vessel formation, as shown in tube formation assays. Further, LY2109761 demonstrated strong antiangiogenic effects *in vivo* as shown by reducing MVD in glioblastoma in mice. Interestingly, LY2109761 also enhanced the fraction of pericyte coverage (α-SMA/CD31 ratio) of tumor vessels alone and in combination with radiotherapy ± chemotherapy. The interpretation of this process as a vascular normalization effect suggests improved physiological conditions for both radiotherapy and chemotherapy, which both depend on functional blood perfusion and/or ample oxygen supply [45]. Because glioblastoma in patients are also highly vascularized and express TGF-β, targeting TGF-β might thus also exhibit antiangiogenic effects in the clinical setting.

These histologic findings are in excellent agreement with quantitative blood perfusion measurements using DCE-MRI. Applying the two-compartment model of Brix et al. [29], DCE-MRI showed a significant decrease of the parameter *amplitude* in all treated groups including the monotherapies, which corresponds to the decrease of MVD under all three monotherapies. This decrease in *amplitude* can be attributed mainly to the reduction of relative blood volume in the tumors [46]. However, combination therapies (both dual and triple) did not further decrease the DCE-MRI *amplitude* value, reflecting a vascular normalization process leading to improved tumor perfusion in agreement with the increased pericyte coverage of the vasculature. For the exchange parameter k_{ep}, which is mainly influenced by vessel permeability, a decrease of k_{ep} could have been expected especially after LY2109761 treatment in analogy to prototypical antiangiogenic agents such as bevacizumab. These antibodies for vascular endothelial growth factor also reduce vascular permeability. However, our results show an increase of k_{ep} after LY2109761 and a basically unchanged k_{ep} after radiation and/or TMZ. Similar effects on k_{ep} after antiangiogenic therapy have been reported in a recent DCE-MRI tumor study [28]. The puzzling finding that antiangiogenics increase k_{ep} may have two possible explanations. First, vessel normalization under antiangiogenic treatment could result in a more laminar flow and thus higher perfusion, which leads to an increase in k_{ep}. Second, therapy-induced apoptosis or other forms of endothelial cell death may increase vessel fenestration and permeability and, consequently, also k_{ep}. Conversely, our finding on DCE-MRI after therapy may have implications for the interpretation of DCE-MRI functional imaging parameters, in particular, in the context of antiangiogenic therapy and tumor vessel normalization.

The angiopoietin ligands (Ang-1 and Ang-2) and their receptor (Tie2) have crucial roles in the tumor angiogenic switch, inflammation, metastasis, and lymphangiogenesis [47]. Increased expression of Ang-2 and higher Ang-2/Ang-1 ratios in tumors correlate with poor prognosis in many cancers. Recent reports have shown that they may

also be involved in vascular normalization of glioblastoma [48]. Tumor vessel normalization effect of LY2109761 suggested by immunohistochemical and DCE-MRI data prompted us to analyze the gene expression of Ang-1 and Ang-2 in tumor cells and study whether their mRNA was modulated by LY2109761 treatment. As expected, LY2109761, alone or in combination with TMZ and/or radiation, was associated with a significant reduction of Ang-2 mRNA, but Ang-1 remained unchanged, thus leading to a decrease in Ang-2/Ang-1 ratios, which may partly account for the vascular normalization effect of LY2109761 observed in our experiment condition.

In summary, the presented preclinical study supports the concept of adding a TGF-βRI inhibitor to radiotherapy ± TMZ regimen in the treatment of glioblastoma. The data suggested that the addition of LY2109761 increased the antitumor effects of radiotherapy ± chemotherapy both *in vivo* and *in vitro*. The beneficial therapeutic effects of LY2109761 are presumably a combination of direct cytotoxic, antimigratory/anti-invasive, and antiangiogenic properties, along with radiosensitizing effects.

Acknowledgments

The authors thank Alexandra Tietz and Thuy Trinh for their excellent technical contributions to the experiments.

References

[1] DeAngelis LM (2001). Brain tumors. *N Engl J Med* **344**, 114–123.
[2] Stupp R, Mason WP, van den Bent MJ, Weller M, Fisher B, Taphoorn MJ, Belanger K, Brandes AA, Marosi C, Bogdahn U, et al. (2005). Radiotherapy plus concomitant and adjuvant temozolomide for glioblastoma. *N Engl J Med* **352**, 987–996.
[3] Derynck R and Zhang YE (2003). Smad-dependent and Smad-independent pathways in TGF-β family signaling. *Nature* **425**, 577–584.
[4] Dumont N and Arteaga CL (2003). Targeting the TGFβ signaling network in human neoplasia. *Cancer Cell* **3**, 531–536.
[5] Jennings MT and Pietenpol JA (1998). The role of transforming growth factor β in glioma progression. *J Neurooncol* **36**, 123–140.
[6] Massagué J (2008). TGF-β in cancer. *Cell* **134**, 215–230.
[7] Seoane J (2006). Escaping from the TGFβ anti-proliferative control. *Carcinogenesis* **27**, 2148–2156.
[8] Wick W, Grimmel C, Wild-Bode C, Platten M, Arpin M, and Weller M (2001). Ezrin-dependent promotion of glioma cell clonogenicity, motility, and invasion mediated by bcl-2 and transforming growth factor-β_2. *J Neurosci* **21**, 3360–3368.
[9] Stiles JD, Ostrow PT, Balos LL, Greenberg SJ, Plunkett R, Grand W, and Heffner RR Jr (1997). Correlation of endothelin-1 and transforming growth factor β-1 with malignancy and vascularity in human gliomas. *J Neuropathol Exp Neurol* **56**, 435–439.
[10] Kjellman C, Olofsson SP, Hansson O, Von Schantz T, Lindvall M, Nilsson I, Salford LG, Sjögren HO, and Widegren B (2000). Expression of TGF-β isoforms, TGF-β receptors, and SMAD molecules at different stages of human glioma. *Int J Cancer* **89**, 251–258.
[11] Jachimczak P, Hessdörfer B, Fabel-Schulte K, Wismeth C, Brysch W, Schlingensiepen KH, Bauer A, Blesch A, and Bogdahn U (1996). Transforming growth factor β mediated autocrine growth regulation of gliomas as detected with phosphorothioate antisense oligonucleotides. *Int J Cancer* **65**, 332–337.
[12] Friess H, Yamanaka Y, Büchler M, Ebert M, Beger HG, Gold LI, and Korc M (1993). Enhanced expression of transforming growth factor β isoforms in pancreatic cancer correlates with decreased survival. *Gastroenterology* **105**, 1846–1856.
[13] von Bernstorff W, Voss M, Freichel S, Schmid A, Vogel I, Jöhnk C, Henne-Bruns D, Kremer B, and Kalthoff H (2001). Systemic and local immunosuppression in pancreatic cancer patients. *Clin Cancer Res* **7**, S925–S932.
[14] Hawinkels LJ, Verspaget HW, van der Reijden JJ, van der Zon JM, Verheijen JH, Hommes DW, Lamers CB, and Sier CF (2009). Active TGF-β_1 correlates with myofibroblasts and malignancy in the colorectal adenoma-carcinoma sequence. *Cancer Sci* **100**, 663–670.
[15] Tsamandas AC, Kardamakis D, Ravazoula P, Zolota V, Salakou S, Tepetes K, Kalogeropoulou C, Tsota I, Kourelis T, Makatsoris T, et al. (2004). The potential role of TGFβ_1, TGFβ_2 and TGFβ_3 protein expression in colorectal carcinomas. *Strahlenther Onkol* **180**, 201–208.
[16] Bruna A, Darken RS, Rojo F, Ocaña A, Peñuelas S, Arias A, Paris R, Tortosa A, Mora J, Baselga J, et al. (2007). High TGFβ-Smad activity confers poor prognosis in glioma patients and promotes cell proliferation depending on the methylation of the PDGF-B gene. *Cancer Cell* **11**, 147–160.
[17] Uhl M, Aulwurm S, Wischhusen J, Weiler M, Ma JY, Almirez R, Mangadu R, Liu YW, Platten M, Herrlinger U, et al. (2004). SD-208, a novel transforming growth factor-β receptor I kinase inhibitor, inhibits growth and invasiveness and enhances immunogenicity of murine and human glioma cells *in vitro* and *in vivo*. *Cancer Res* **64**, 7954–7961.
[18] Ge R, Rajeev V, Ray P, Lattime E, Rittling S, Medicherla S, Protter A, Murphy A, Chakravarty J, Dugar S, et al. (2006). Inhibition of growth and metastasis of mouse mammary carcinoma by selective inhibitor of transforming growth factor-β type I receptor kinase *in vivo*. *Clin Cancer Res* **12**, 4315–4330.
[19] Zhang B, Halder SK, Zhang S, and Datta PK (2009). Targeting transforming growth factor-β signaling in liver metastasis of colon cancer. *Cancer Lett* **277**, 114–120.
[20] Melisi D, Ishiyama S, Sclabas GM, Fleming JB, Xia Q, Tortora G, Abbruzzese JL, and Chiao PJ (2008). LY2109761, a novel transforming growth factor β receptor type I and type II dual inhibitor, as a therapeutic approach to suppressing pancreatic cancer metastasis. *Mol Cancer Ther* **7**, 829–840.
[21] Fransvea E, Angelotti U, Antonaci S, and Giannelli G (2008). Blocking transforming growth factor-β up-regulates E-cadherin and reduces migration and invasion of hepatocellular carcinoma cells. *Hepatology* **47**, 1557–1566.
[22] Andarawewa KL, Paupert J, Pal A, and Barcellos-Hoff MH (2007). New rationales for using TGFβ inhibitors in radiotherapy. *Int J Radiat Biol* **83**, 803–811.
[23] Kirshner J, Jobling MF, Pajares MJ, Ravani SA, Glick AB, Lavin MJ, Koslov S, Shiloh Y, and Barcellos-Hoff MH (2006). Inhibition of transforming growth factor-β_1 signaling attenuates ataxia telangiectasia mutated activity in response to genotoxic stress. *Cancer Res* **66**, 10861–10869.
[24] Park CM, Park MJ, Kwak HJ, Lee HC, Kim MS, Lee SH, Park IC, Rhee CH, and Hong SI (2006). Ionizing radiation enhances matrix metalloproteinase-2 secretion and invasion of glioma cells through Src/epidermal growth factor receptor–mediated p38/Akt and phosphatidylinositol 3-kinase/Akt signaling pathways. *Cancer Res* **66**, 8511–8519.
[25] Wild-Bode C, Weller M, Rimner A, Dichgans J, and Wick W (2001). Sublethal irradiation promotes migration and invasiveness of glioma cells: implications for radiotherapy of human glioblastoma. *Cancer Res* **61**, 2744–2750.
[26] Pepper MS (1997). Transforming growth factor-β: vasculogenesis, angiogenesis, and vessel wall integrity. *Cytokine Growth Factor Rev* **8**, 21–43.
[27] Almog N, Ma L, Raychowdhury R, Schwager C, Erber R, Short S, Hlatky L, Vajkoczy P, Huber PE, Folkman J, et al. (2009). Transcriptional switch of dormant tumors to fast-growing angiogenic phenotype. *Cancer Res* **69**, 836–844.
[28] Zwick S, Strecker R, Kiselev V, Gall P, Huppert J, Palmowski M, Lederle W, Woenne EC, Hengerer A, Taupitz M, et al. (2009). Assessment of vascular remodeling under antiangiogenic therapy using DCE-MRI and vessel size imaging. *J Magn Reson Imaging* **29**, 1125–1133.
[29] Brix G, Semmler W, Port R, Schad LR, Layer G, and Lorenz WJ (1991). Pharmacokinetic parameters in CNS Gd-DTPA enhanced MR imaging. *J Comput Assist Tomogr* **15**, 621–628.
[30] Hammond LA, Eckardt JR, Baker SD, Eckhardt SG, Dugan M, Forral K, Reidenberg P, Statkevich P, Weiss GR, Rinaldi DA, et al. (1999). Phase I and pharmacokinetic study of temozolomide on a daily-for-5-days schedule in patients with advanced solid malignancies. *J Clin Oncol* **8**, 2604–2613.
[31] Arpino G, Gutierrez C, Weiss H, Rimawi M, Massarweh S, Bharwani L, De Placido S, Osborne CK, and Schiff R (2007). Treatment of human epidermal growth factor receptor 2–overexpressing breast cancer xenografts with multiagent HER-targeted therapy. *J Natl Cancer Inst* **99**, 694–705.
[32] Yoshino A, Ogino A, Yachi K, Ohta T, Fukushima T, Watanabe T, Katayama Y, Okamoto Y, Naruse N, Sano E, et al. (2010). Gene expression profiling predicts response to temozolomide in malignant gliomas. *Int J Oncol* **36**, 1367–1377.
[33] Chalmers AJ, Ruff EM, Martindale C, Lovegrove N, and Short SC (2009). Cytotoxic effects of temozolomide and radiation are additive- and schedule-dependent. *Int J Radiat Oncol Biol Phys* **75**, 1511–1519.
[34] Chakravarti A, Erkkinen MG, Nestler U, Stupp R, Mehta M, Aldape K, Gilbert MR, Black PM, and Loeffler JS (2006). Temozolomide-mediated radiation

enhancement in glioblastoma: a report on underlying mechanisms. *Clin Cancer Res* **12**, 4738–4746.

[35] Hegi ME, Diserens AC, Gorlia T, Hamou MF, de Tribolet N, Weller M, Kros JM, Hainfellner JA, Mason W, Mariani L, et al. (2005). MGMT gene silencing and benefit from temozolomide in glioblastoma. *N Engl J Med* **352**, 997–1003.

[36] Mariani L, Beaudry C, McDonough WS, Hoelzinger DB, Kaczmarek E, Ponce F, Coons SW, Giese A, Seiler RW, and Berens ME (2001). Death-associated protein 3 (Dap-3) is overexpressed in invasive glioblastoma cells *in vivo* and in glioma cell lines with induced motility phenotype *in vitro*. *Clin Cancer Res* **7**, 2480–2489.

[37] Cho SY and Klemke RL (2000). Extracellular regulated kinase activation and CAS/Crk coupling regulate cell migration and suppress apoptosis during invasion of the extracellular matrix. *J Cell Biol* **149**, 223–236.

[38] Qian LW, Mizumoto K, Urashima T, Nagai E, Maehara N, Sato N, Nakajima M, and Tanaka M (2002). Radiation-induced increase in invasive potential of human pancreatic cancer cells and its blockade by a matrix metalloproteinase inhibitor, CGS27023. *Clin Cancer Res* **8**, 1223–1227.

[39] Merzak A, McCrea S, Koocheckpour S, and Pilkington GJ (1994). Control of human glioma cell growth, migration and invasion *in vitro* by transforming growth factor β_1. *Br J Cancer* **70**, 199–203.

[40] Hjelmeland MD, Hjelmeland AB, Sathornsumetee S, Reese ED, Herbstreith MH, Laping NJ, Friedman HS, Bigner DD, Wang XF, and Rich JN (2004). SB-431542, a small molecule transforming growth factor-β-receptor antagonist, inhibits human glioma cell line proliferation and motility. *Mol Cancer Ther* **3**, 737–745.

[41] Dings RP, Loren M, Heun H, McNiel E, Griffioen AW, Mayo KH, and Griffin RJ (2007). Scheduling of radiation with angiogenesis inhibitors anginex and avastin improves therapeutic outcome via vessel normalization. *Clin Cancer Res* **13**, 3395–3402.

[42] Wachsberger PR, Burd R, Marero N, Daskalakis C, Ryan A, McCue P, and Dicker AP (2005). Effect of the tumor vascular-damaging agent, ZD6126, on the radioresponse of U87MG glioblastoma. *Clin Cancer Res* **11**, 835–842.

[43] Koochekpour S, Merzak A, and Pilkington GJ (1996). Vascular endothelial growth factor production is stimulated by gangliosides and TGFβ isoforms in human glioma cells *in vitro*. *Cancer Lett* **102**, 209–215.

[44] Platten M, Wick W, Wild-Bode C, Aulwurm S, Dichgans J, and Weller M (2000). Transforming growth factors β_1 (TGF-β_1) and TGF-β_2 promote glioma cell migration via up-regulation of $\alpha_V\beta_3$ integrin expression. *Biochem Biophys Res Commun* **268**, 607–611.

[45] Jain RK (2005). Normalization of tumor vasculature: an emerging concept in antiangiogenic therapy. *Science* **307**, 58–62.

[46] Kiessling F, Krix M, Heilmann M, Vosseler S, Lichy M, Fink C, Farhan N, Kleinschmidt K, Schad L, Fusenig NE, et al. (2003). Comparing dynamic parameters of tumor vascularization in nude mice revealed by magnetic resonance imaging and contrast-enhanced intermittent power Doppler sonography. *Invest Radiol* **38**, 516–524.

[47] Huang H, Bhat A, Woodnutt G, and Lappe R (2010). Targeting the ANGPT-TIE2 pathway in malignancy. *Nat Rev Cancer* **10**, 575–585.

[48] Chae SS, Kamoun WS, Farrar CT, Kirkpatrick ND, Niemeyer E, de Graaf AM, Sorensen AG, Munn LL, Jain RK, and Fukumura D (2010). Angiopoietin-2 interferes with anti–VEGFR2-induced vessel normalization and survival benefit in mice bearing gliomas. *Clin Cancer Res* **16**, 3618–3627.

Table W1. Radiation Doses That Reduce Cell Clonogenic Survival to 10% (D0.1) Calculated by Fitting the Linear Quadratic Equation to Clonogenic Survival after Treatment with Radiation Alone and in Combination with LY2109761 and/or TMZ.

Cell	Treatment	D0.1 (Gy)	DEF
U87MG	RT alone	7.03	
	RT + Ly	5.44	1.29
	RT + TMZ	5.76	1.22
	RT + Ly + TMZ	4.67	1.51
T98	RT alone	6.15	
	RT + Ly	4.97	1.24
	RT + TMZ	6.09	1.01
	RT + Ly + TMZ	4.90	1.26

Dose enhancement factor (DEF) was defined as the quotient of D0.1 RT/D0.1 RT + drug(s). DEF greater than 1 indicates greater than independent toxicity in combined treatment.
Ly indicates LY2109761.

Table W2. Effects of Each Treatment on TTP of U87MG and T98 Tumor Xenografts.

Tumor Model	Group	TTP (Mean ± SD; Days)	TTP Control (Days)
U87MG	Control	11.1 ± 1.79	
	Ly	32.0 ± 6.28	20.9
	TMZ	64.3 ± 9.14	53.2
	RT	29.7 ± 7.17	18.6
	Ly + TMZ	79.9 ± 7.15	68.8
	Ly + RT	62.1 ± 8.29	53.8
	TMZ + RT	75.4 ± 8.29	64.3
	Ly + TMZ + RT	95.9 ± 2.39	84.8
T98	Control	10.1 ± 1.26	
	Ly	16.5 ± 2.53	6.4
	TMZ	11.9 ± 1.58	1.8
	RT	20.9 ± 4.32	10.8
	Ly + TMZ	18.1 ± 4.41	8.0
	Ly + RT	30.8 ± 6.16	20.7
	TMZ + RT	22.6 ± 5.07	12.5
	Ly + TMZ + RT	34.3 ± 7.13	24.2

TTP is defined as the time when tumor volume increased three times from the baseline value for each mouse. TTP control is defined as TTP difference between each treatment group and control group.
Ly indicates LY2109761.